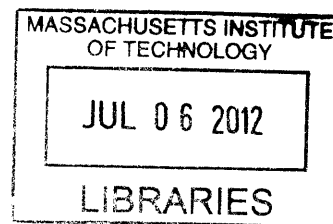


Microneedle delivery for improved efficacy of antiretroviral and antibiotic drugs

by

Zachary Jason Stauber



Submitted to the Department of Materials Science and Engineering in Partial Fulfillment of the Requirements for the Degree of Bachelor of Science at the Massachusetts Institute of Technology

May 2012

© 2012 Zachary Jason Stauber

All rights reserved

The author hereby grants to MIT permission to reproduce and to distribute publicly paper and electronic copies of this thesis document in whole or in part in any medium now known or hereafter created

Signature of author \_\_\_\_\_

Handwritten signature of Zachary Stauber in black ink.

Zachary Stauber

Department of Materials Science and Engineering

May 11, 2012

Certified by \_\_\_\_\_

Handwritten signature of Darrell J. Irvine in black ink.

Darrell J. Irvine

Associate Professor of MSE and Biological Engineering

Thesis Supervisor

Accepted by \_\_\_\_\_

Handwritten signature of Jeffrey Grossman in black ink.

Jeffrey Grossman

Associate Professor of MSE and Mechanical Engineering

Chairman, Undergraduate Thesis Committee

# Microneedle delivery for improved efficacy of antiretroviral and antibiotic drugs

by

Zachary Jason Stauber

Submitted to the Department of Materials Science and Engineering on May 11, 2012 in Partial Fulfillment of the Requirements for the Degree of Bachelor of Science at the Massachusetts Institute of Technology

## Abstract

Two classes of drugs, antiretrovirals and antibiotics, could benefit greatly from delivery through microneedles. Microneedles (MN) offer an increase in efficacy for these drugs by providing delivery to the lymphatic system through the skin, thus avoiding first pass metabolism and allowing more focused delivery to specific viral or bacterial reservoirs. Furthermore, microneedles present other advantages in the form of the ability to be self-administered, tunable controlled release, and painless administration. Saquinavir and Ciprofloxacin, an antiretroviral and an antibiotic respectively, were chosen for their optimal properties, including bioavailability, half-life, and dosage. Saquinavir was encapsulated in the organic phase of biodegradable poly(lactide-*co*-glycolide) microparticles (MP) synthesized through a double emulsion. Similarly, Ciprofloxacin was encapsulated in the aqueous phase of the microparticles. In addition, Ciprofloxacin microcrystals were synthesized. The microparticles and microcrystals were then loaded into molded polymer microneedles in a poly-acrylic acid (PAA) matrix. Standard curves were created for the two drugs from known concentrations and used to show the drug loading in the microparticles and microneedles. The Saquinavir microparticles showed a maximum loading of 1.35% the mass of particles and the Ciprofloxacin microparticles showed a maximum loading of 0.197%. The Saquinavir microparticle microneedles had a maximum loading of 11.95  $\mu\text{g}$  of Saquinavir per 1  $\text{cm}^2$  array and the Ciprofloxacin microparticle microneedles had a maximum loading of .41  $\mu\text{g}$  of Ciprofloxacin per 1  $\text{cm}^2$  array. The Ciprofloxacin microcrystal microneedles had a maximum loading of 165  $\mu\text{g}$  per 1  $\text{cm}^2$  array. Analysis based on insulin delivery through microneedles showed these loadings to be too low to create the sufficient minimum drug concentration in plasma. However, there exist multiple strategies to increase the loading of the drugs in the microneedles. These results proved promising for the use of microneedles for the delivery of antiretroviral and antibiotic drugs.

Thesis Supervisor: Darrell J. Irvine

Title: Associate Professor of MSE and Biological Engineering

## Table of figures

Figure 1: Envisioned application and delivery of drug through microneedles.....	9
Figure 2: Outline of work accomplished. Shown are microparticles (MPs), microcrystals (MCs) and microneedles (MN) .....	12
Figure 3: The structure of Saquinavir in the mesylate form, obtained from Sigma Aldrich <sup>28</sup> ....	15
Figure 4: The structure of Maraviroc, obtained from Sigma Aldrich <sup>30</sup> .....	16
Figure 5: Microparticle synthesis outline. ....	18
Figure 6: Microparticles with drug loaded in the organic phase .....	19
Figure 7: Outline of the microneedle fabrication process.....	24
Figure 8: PDMS mold used to synthesize microneedles .....	26
Figure 9: Saquinavir Standard Curve for with error bars from 3 series of measurements .....	29
Figure 10: From Ha et al, the UV-spectrum of Saquinavir-mesylate dissolved in .01M HCl <sup>25</sup> ...	30
Figure 11: Maraviroc standard curve at 257 nm zeroed with .2M NaOH + varying levels of DMSO to match the concentration present in Maraviroc samples. Error bars derived from replicate measurement zeroed only in 0.2M NaOH.....	30
Figure 12: Correlation shown graphically and approximated as linear between increase in loading during synthesis and actual loading. No error analysis available due to absence of replication measurements.....	33
Figure 13: On the left, the Saquinavir microparticle loaded microneedles and on the right, a higher magnification image of a control microparticle loaded microneedle. ....	34
Figure 14: The structure of Ciprofloxacin, obtained from Sigma Aldrich. <sup>36</sup> .....	37
Figure 15: Microparticles with drug loaded in the internal aqueous phase .....	38
Figure 16: Ciprofloxacin standard curve, checked with multiple dilutions at different pH as well as solution in 0.2M NaOH. Error bars derived from replicate measurements of different starting concentrations (10 mg/mL and 30 mg/mL) .....	41
Figure 17: From top left to right: 30 mg/mL Cipro MP MN, 10 mg/mL Cipro MP MN; bottom left to right: sonicated ciprofloxacin microcrystal MN, precipitated ciprofloxacin microcrystal MN .....	45

**Table of tables**

<b>Table 1: Drug properties for Saquinavir and Maraviroc used to select candidate drugs .....</b>	<b>15</b>
<b>Table 2: Characterization results for Saquinavir loaded particles, above, and the control particles, below.....</b>	<b>32</b>
<b>Table 3: The correlation between loading ratio during synthesis and actual loading of microparticles.....</b>	<b>33</b>
<b>Table 4: Drug properties for Ciprofloxacin that were used to select it as a candidate drug .....</b>	<b>37</b>
<b>Table 5: Characterization of ciprofloxacin loaded microparticles with different loading levels .</b>	<b>42</b>
<b>Table 6: Different predicted and actual loadings for different concentrations of Ciprofloxacin in the internal aqueous phase .....</b>	<b>43</b>

# Contents

<b>Abstract .....</b>	<b>2</b>
<b>Table of figures.....</b>	<b>3</b>
<b>Table of tables .....</b>	<b>4</b>
<b>I INTRODUCTION.....</b>	<b>7</b>
<b>a. Background.....</b>	<b>7</b>
<b>b. Scope of work.....</b>	<b>10</b>
<b>II MICRONEEDLE DELIVERY OF ANTIRETROVIRAL DRUGS.....</b>	<b>13</b>
<b>a. Introduction .....</b>	<b>13</b>
<b>b. Materials and methods .....</b>	<b>14</b>
i. Drug Choice .....	14
ii. Standard curves .....	16
1. <i>Saquinavir</i> .....	16
2. <i>Maraviroc</i> .....	16
iii. Microparticle synthesis.....	17
1. <i>Organic phase preparation</i> .....	19
2. <i>Aqueous phase preparations</i> .....	20
3. <i>Particle preparation and work-up</i> .....	20
4. <i>Particle Characterization</i> .....	22
iv. Microparticle loading .....	22
v. Microneedle synthesis and characterization .....	23
1. <i>PDMS microneedle mold fabrication</i> .....	25
2. <i>Microparticle deposition</i> .....	26
3. <i>Polyacrylic acid addition</i> .....	27
vi. Microneedle loading.....	27
<b>c. Results and discussion .....</b>	<b>28</b>
i. Standard curves .....	28
ii. Microparticles.....	31
iii. Microparticle loading .....	32
iv. Microneedles .....	33
v. Microneedle loading.....	34
<b>d. Conclusion.....</b>	<b>35</b>
<b>III. MICRONEEDLE DELIVERY OF ANTIBIOTICS.....</b>	<b>36</b>

<b>a.</b>	<b>Introduction .....</b>	<b>36</b>
<b>b.</b>	<b>Materials and Methods .....</b>	<b>36</b>
i.	Drug Choice .....	37
ii.	Standard curves .....	37
iii.	Microparticle synthesis.....	38
1.	<i>Organic phase preparation.....</i>	<i>39</i>
2.	<i>Aqueous phase preparations.....</i>	<i>39</i>
3.	<i>Particle preparation and work-up.....</i>	<i>39</i>
4.	<i>Particle characterization.....</i>	<i>39</i>
iv.	Microparticle loading .....	39
v.	Microcrystals .....	40
vi.	Microneedle synthesis and characterization .....	40
vii.	Microneedle loading.....	40
<b>c.</b>	<b>Results and discussion .....</b>	<b>41</b>
i.	Standard curve.....	41
ii.	Microparticles.....	41
iii.	Microparticle loading .....	43
iv.	Microcrystals .....	43
v.	Microneedles .....	44
vi.	Microneedle loading.....	45
<b>d.</b>	<b>Conclusion.....</b>	<b>46</b>
<b>IV.</b>	<b>CONCLUSION.....</b>	<b>48</b>
<b>a.</b>	<b>Summary.....</b>	<b>48</b>
<b>b.</b>	<b>Future work.....</b>	<b>48</b>
	<b>Acknowledgments.....</b>	<b>50</b>
	<b>Works cited.....</b>	<b>51</b>

# **I Introduction**

## **a. Background**

Drug delivery has become an increasingly important field with continued advances in drug discovery. Just as important as how the drug acts is how it is delivered. Historically, drugs have been delivered into the human body through two main forms: orally through pills and directly into the bloodstream through hypodermic injections<sup>1</sup>. Controlled release transdermal drug delivery offers numerous benefits over the aforementioned forms of drug delivery. Drug patches and microneedles (MN) are two methods for transdermal delivery that have been thoroughly investigated<sup>2,3</sup>. The drug patches are limited to only a handful of drugs, while microneedles have the capability to be much more universal in the drugs they can introduce<sup>1</sup>.

Orally delivered drugs must traverse the digestive system, which can lead to a loss of drug as it is absorbed across the intestinal wall as well as losses due to the first pass effect from the liver metabolizing the drug<sup>2</sup>. The drug must also be able to remain intact after being exposed to the harsh environment of the digestive system, including acidity of the stomach and numerous enzymes throughout the intestines<sup>1</sup>. The drug's charge and solubility affect the absorption the drug's absorption and create an extra parameter in designing the drug. Finally, the drug can cause side effects to the digestive system and is susceptible to a varied digestive environment dependent on other foods in the digestive system<sup>2</sup>.

Hypodermic injections, including intravenous (IV), intramuscular, subcutaneous, and intradermal injections, eliminate many of these problems because they bypass the digestive system and the drug is delivered directly into the bloodstream. These injections, however, are more invasive and have a number of undesired characteristics<sup>4</sup>. Improper maintenance and use

of needles can also lead to infections<sup>4</sup>. The needles used for injections can become dangerous medical waste and pose the danger of transmitting diseases through shared needle use, which is prevalent in developing and poverty stricken nations<sup>1,2</sup>. Administering these injections usually requires special training and expertise (e.g. finding a vein for IV injection or using correct angle for subcutaneous injections).

Transdermal delivery is a further improvement on injections; it bypasses the digestive system, but doesn't have the drawbacks or pose the dangers that other types of injections do. Transdermal delivery was first developed as a patch loaded with the drug that would diffuse across the stratum corneum into the skin over time<sup>1</sup>. The most well known example is the Nicoderm CQ patch, which introduces nicotine into the patient at gradually smaller amounts to help the user quit smoking. However, due to the low permeability of the skin, only small drug molecules (molecular masses of up to a few hundred Daltons) with specific octanol-water partition coefficients can be used to deliver therapeutic doses with patches<sup>1,2</sup>. These limitations rule out many hydrophilic drugs, as well as macromolecules, such as DNA and peptide drugs. Thus microneedles are an advantageous form of transdermal delivery since they can be used for a larger variety of drugs and more efficiently transmit the drug; instead of relying on diffusion for the drug to pass the outer skin layer, microneedles physically place the drug into the body. A huge benefit of delivering drugs transdermally is the ability to access the epidermal and top of the dermal layer of the skin. This means that the microneedles are short enough to avoid the nerve endings and therefore not cause pain, while also accessing certain immune cells that are critical to the drug efficacy<sup>5</sup>. Langerhans cells, which are present in the epidermal layer, are susceptible to human immunodeficiency virus (HIV) infection and are known to be viral



reservoirs of dissemination<sup>4</sup>. By directly targeting these viral reservoirs, anti-HIV therapies could be more effective.

**Figure 1** below gives the envisioned application of delivery of the drug using the microneedles. The solid PAA matrix of the polyacrylic acid (PAA) microneedles encapsulate either drug crystals or drugs suspended in poly(lactide-*co*-glycolide) (PLGA) microparticles. The microneedles are inserted into the epidermal or dermal layers of the skin to release the drug. The PAA matrix dissolves when it comes in contact with the water based skin fluids, releasing either the drug crystals or the drug microparticles. The drug crystals become soluble in the skin fluid due to low concentrations and potentially due to a change in pH and the PLGA matrix of the drug microparticles similarly dissolves in the water based skin fluid, releasing the drug. The drug is then able to diffuse to key areas of interest.

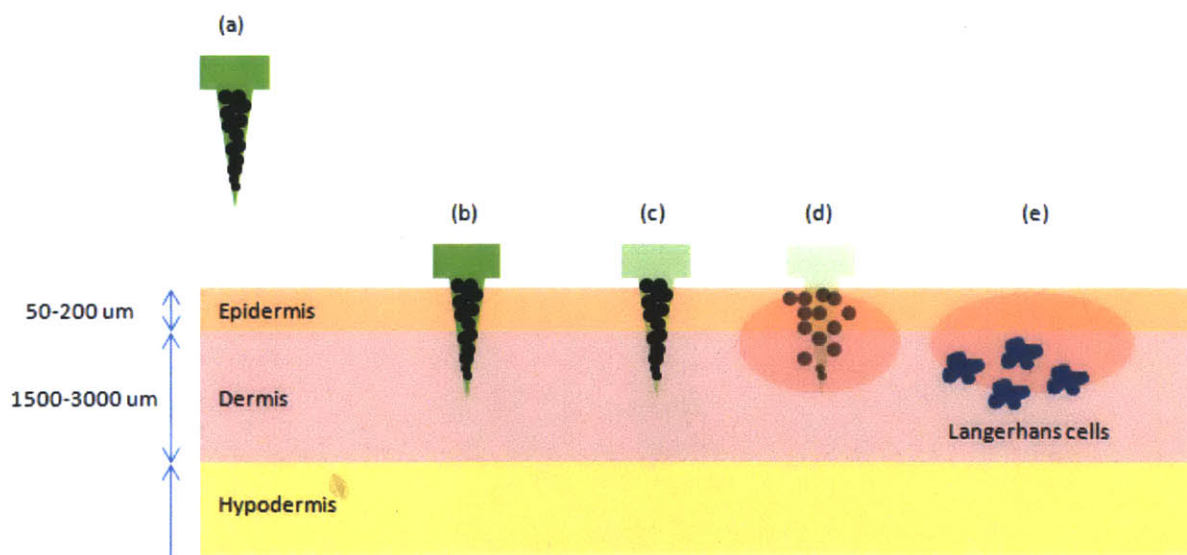


Figure 1: Envisioned application and delivery of drug through microneedles. (a) Microneedles are synthesized with polyacrylic acid (PAA) base with either microparticles or microcrystals suspended in matrix of PAA (b) microneedles are inserted into the skin and access the top layer of the dermis or bottom of epidermis depending on size of microneedles and application strength (c) PAA matrix begins to dissolve due to hydrolysis from water in body (d) most of matrix is dissolved and microparticles release drug or microcrystals dissolve due to pH (e) Complete

dissolution of microneedle and microparticles or microcrystals leaving dissolved drug to diffuse away to areas of interest, including lymphatic cells such as Langerhans cells

## **b. Scope of work**

This paper investigates the use of microneedles as a plausible mechanism for drug delivery. Two classes of drugs are examined because of the potential increase of efficacy with these drugs by using microneedles. Antiretroviral and antibiotic drugs are hypothesized to greatly benefit from delivery using microneedles due to the access of particular immune cells in the epidermal layer as well as bypassing first pass metabolism, in addition to painless, self-administered delivery.

This work builds upon previous work that has investigated microneedle use for vaccine delivery. Therefore, certain protocols have already been established and certain parameters optimized. There still exist a variety of parameters to optimize, including the form of the drug loaded into the microneedle. This affects the amount of drug that can be loaded into a single microneedle array as well as delivery rates of the drug. Microparticles, where the drug was embedded in a matrix of PLGA, and microcrystals, pure crystalline drug, were both investigated as possible methods for drug encapsulation. Microparticles would have more controllable drug release rates, while microcrystals allow for higher loading levels. Other encapsulation methods, such as using reservoirs and coating the microneedle surfaces, also exist that can be investigated in future studies.

An outline of the work achieved is shown in **Figure 2**, below. Two candidate drugs, Maraviroc and Saquinavir, were used to demonstrate the ability to encapsulate antiretroviral drugs in microneedles while Ciprofloxacin was used to demonstrate the ability to similarly encapsulate antibiotic drugs. A standard curve was created for each drug, followed by synthesis

of drug microparticles and drug microcrystals. The microparticles were then tested for loading and both the microparticles and microcrystals were encapsulated in microneedles. These microneedles were then tested for loading to demonstrate the ability to encapsulate drugs in microneedles.

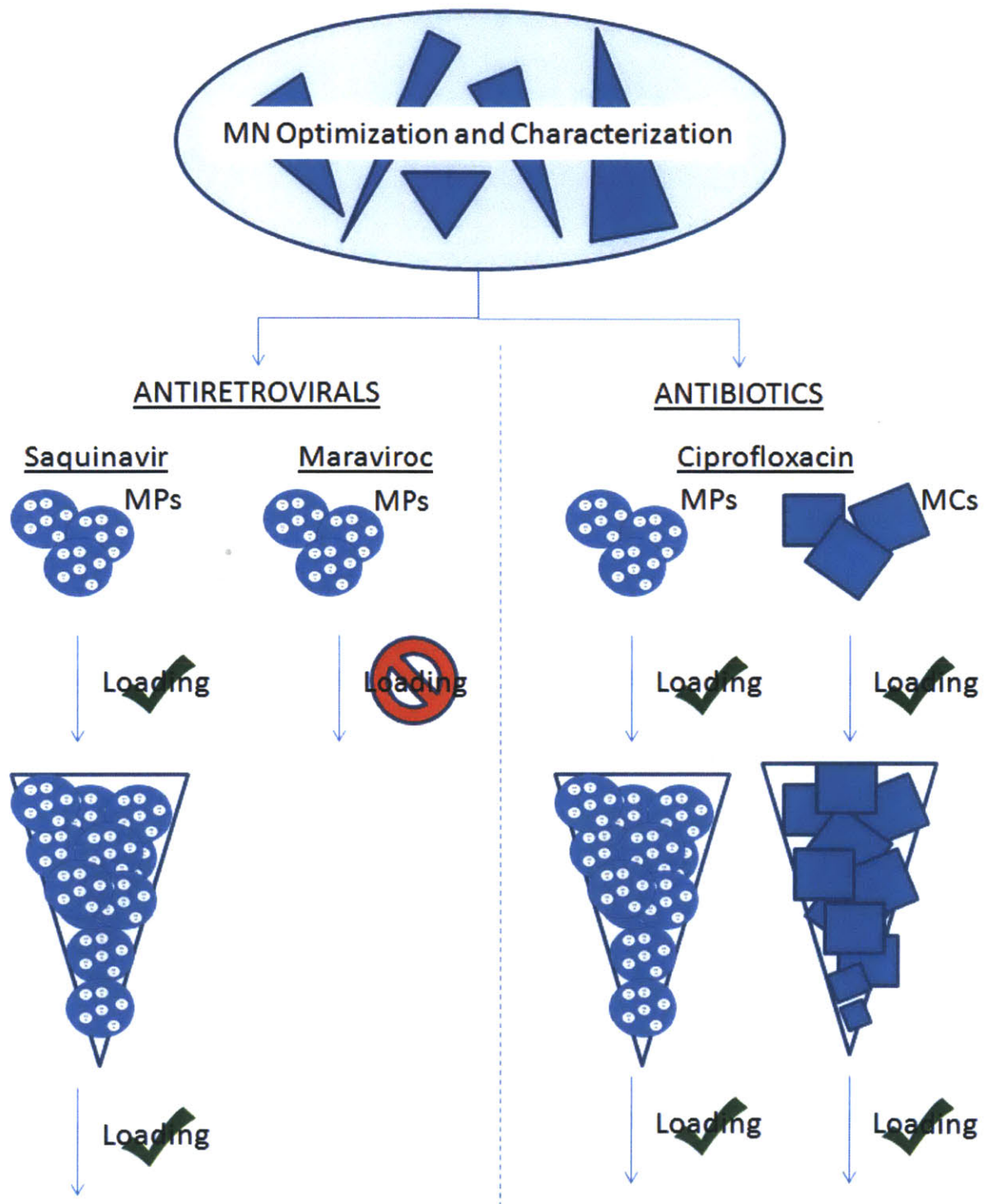


Figure 2: Outline of work accomplished. Shown are microparticles (MPs), microcrystals (MCs) and microneedles (MN)

## **II Microneedle Delivery of Antiretroviral Drugs**

### **a. Introduction**

In 2009, HIV infected an estimated 36 million people worldwide, with the vast majority of those infected living in developing nations with limited access to treatment resources<sup>9</sup>. Current antiretroviral (AR) therapies have proven to be highly effective in controlling HIV replication and consequently increase the life expectancy of patients. These therapies, however, require frequent and high doses and have a number of undesirable side effects, all of which lead to patient incompliance. In addition, in order to be effective, compliance above 95% is needed, below which, the AR effectiveness can drop as much as 50%<sup>10,11</sup>. AR therapies also do not fully eliminate the virus from the host and are unable to remove viral reservoirs. Therefore, a drug delivery method that decreases dose amount and frequency and improves patient incompliance as well as targets viral reservoirs would be a drastic improvement over current methods. Microneedles are able to access these viral reservoirs and would decrease the dosage required since they deliver drugs directly into the epidermal layer of the skin and completely bypass the digestive tract. In addition, they can be tuned for desired controlled release rates, allowing for a sustained critical effective level of drug, a major benefit over the large variations in drug concentrations with pills.

A number of factors were used in determining candidate drugs. Drugs which could benefit maximally from microneedle delivery would have low half-lives, high potency, low bioavailabilities, and require frequent doses. Microneedles would have the most improvement in efficacy with drugs with these characteristics because microneedles are able to replace frequent doses with controlled release strategies and are able to effectively deliver drugs, overcoming low

bioavailability. High potency is desirable because of the limitation of microneedles for delivering large amounts of drug due to their size. For the 650  $\mu\text{m}$  height and 250  $\mu\text{m}$  width microneedles we fabricated, this results in  $\sim 1 \mu\text{L}$  per microneedle, which is approximately .012 mg of Saquinavir with a density of  $1.2 \text{ g/cm}^3$  assuming 100% loading of pure Saquinavir<sup>12</sup>. The microneedle arrays have 78 microneedles, indicating a maximum of 0.94 mg of Saquinavir per array.

Microparticles allow for tunable controlled release of the drug. They are essentially encapsulating the drug in a biodegradable matrix with a known hydrolysis rate. Once the microparticles enter the body, they would mostly remain localized due to their size and release the drug to be taken up into systemic circulation. At low levels, the microparticles might be carried to the draining lymph nodes by antigen presenting cells, releasing the drug directly to the lymph nodes.

## **b. Materials and methods**

### **i. Drug Choice**

**Table 1** below shows the two drugs chosen as candidate drugs based on the desired characteristics. Bioavailability is defined as the amount of drug that reaches the systemic circulation. Terminal half life is the amount of time to reduce plasma concentrations by half while elimination half life is the amount of time it takes for the drug to lose half of its pharmacological activity.

<i>Drug name</i>	<i>Bioavailability</i>	<i>Half-life (hours)</i>	<i>Dose frequency (doses/day)</i>	<i>Total Daily Dosage (mg)</i>	<i>Minimum effective concentration (ng/mL)</i>

Saquinavir	.4% to 5% <sup>13</sup>	Terminal: 10-12 <sup>14</sup> Elimination: 1-3 <sup>15,16</sup>	2-5 <sup>17</sup>	1000-1200 <sup>17</sup>	100 <sup>19</sup>
Maraviroc	23% <sup>21</sup>	Terminal: 14-18 <sup>22</sup> Elimination: 10.6 <sup>23</sup>	2 <sup>20</sup>	1200 <sup>20</sup>	25 <sup>24</sup>

Table 1: Drug properties for Saquinavir and Maraviroc used to select candidate drugs

Saquinavir is a potent protease inhibitor that is available in two forms, as a soft-gel capsule with trade name Fortovase, and in the form of a salt, Saquinavir-mesylate, with the trade name Invirase. The latter, Saquinavir-mesylate, was obtained from Sigma-Aldrich, with structure shown below in **Figure 3**.

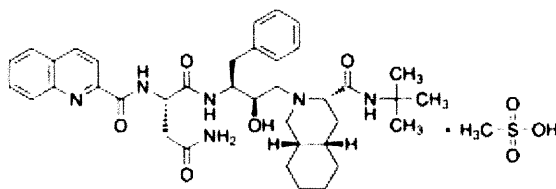


Figure 3: The structure of Saquinavir in the mesylate form, obtained from Sigma Aldrich<sup>28</sup>

Maraviroc is a potent antiretroviral entry inhibitor, acting as a CCR5 chemokine receptor antagonist. It is sold with the trade name Selzentry and was also obtained from Sigma-Aldrich. Its structure is shown below in **Figure 4**.

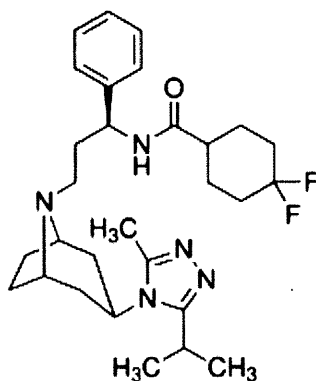


Figure 4: The structure of Maraviroc, obtained from Sigma Aldrich<sup>30</sup>

## ii. Standard curves

In order to determine concentrations of drugs, standard curves were created for both Maraviroc and Saquinavir. Using a Thermo-Scientific Multiskan GO ultraviolet-visible (UV) spectrophotometer, samples of known concentration were created and the intensity of the peak absorption of these concentrations was used to create a standard curve.

### 1. *Saquinavir*

Saquinavir has a low aqueous solubility of 2.22 mg/mL and was dissolved in dimethylsulfoxide (DMSO) at 5 mg/mL, the solubility in DMSO according to Sigma<sup>27,28</sup>. To control for the fact that sodium hydroxide (NaOH) would be used to hydrolyze the microparticles and microneedles, the dilutions were made in 0.2 M NaOH. In addition, due to the UV absorbance of the polystyrene disposable cuvettes, a Starna Cells quartz open top 10 mm cuvette was used to eliminate any false signals from the polystyrene cuvettes. The UV spectrophotometer was set to quick read from 200 nm to 450 nm.

### 2. *Maraviroc*



Maraviroc also has a low aqueous solubility and was initially dissolved at 30 mg/mL, the solubility according to Sigma <sup>30</sup>. Similarly, the dilutions were made in 0.2 M NaOH to control for the NaOH that would be used to hydrolyze the microparticles and microneedles. The quartz cuvette was used in favor of the disposable polystyrene cuvette as soon as it was discovered that the polystyrene cuvettes were giving false signals and had strong absorption in the UV range, particularly at the wavelengths of interest. The UV spectrophotometer was set to quick read from 200 nm to 450 nm.

iii. Microparticle synthesis

The microparticle synthesis is a double emulsion synthesis that requires multiple steps in order to encapsulate drug in particles of micron diameter. **Figure 5** below, outlines these various steps.

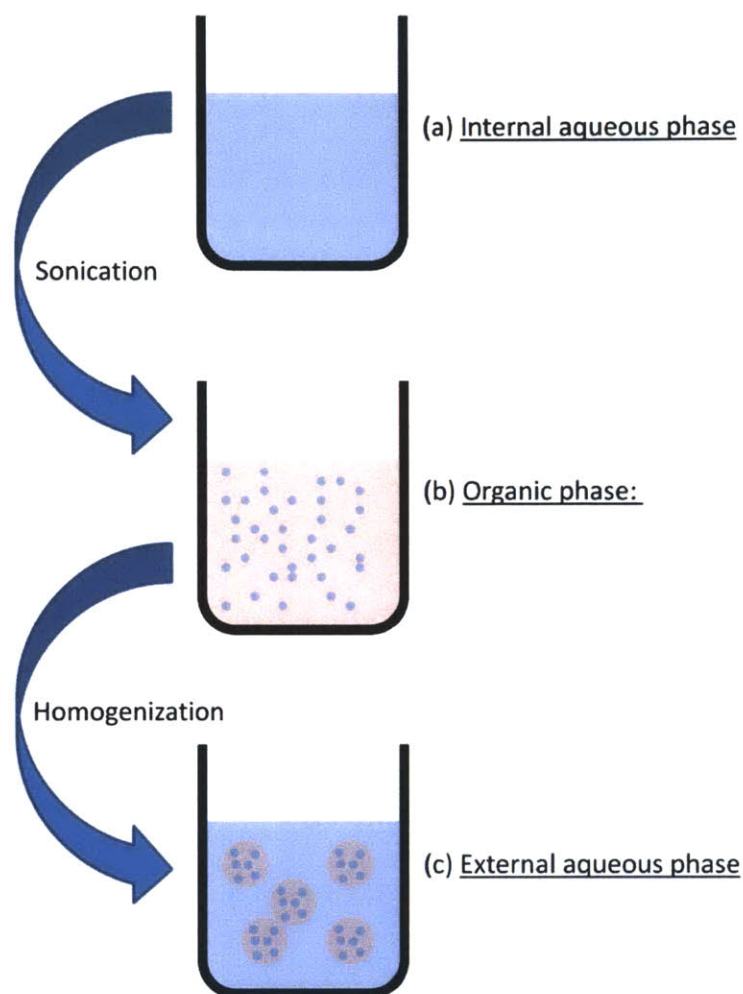


Figure 5: Microparticle synthesis outline. (a) The internal aqueous phase, drug could be loaded here, is sonicated as it is added to an organic phase (b) The internal aqueous phase therefore forms nanoparticles in the organic phase, which could also be loaded with drug (c) The organic phase with nanoparticles of the internal aqueous phase is then added to an external aqueous phase as the external aqueous phase is homogenized. (c) The organic phase-internal aqueous phase then forms microparticles in the external aqueous phase

For reasons discussed below in results and discussion, only Saquinavir was continued as a candidate drug due to impracticality of measuring concentrations of Maraviroc. However, a control was also created with the exact same synthesis, but without the addition of the

Saquinavir. Saquinavir was encapsulated into microparticles that would act as the controlled release mechanism. The microparticle synthesis was a double emulsion synthesis where an internal aqueous phase was suspended in an organic phase, which was then suspended in a second external aqueous phase. **Figure 6** shows the structure of the microparticles.

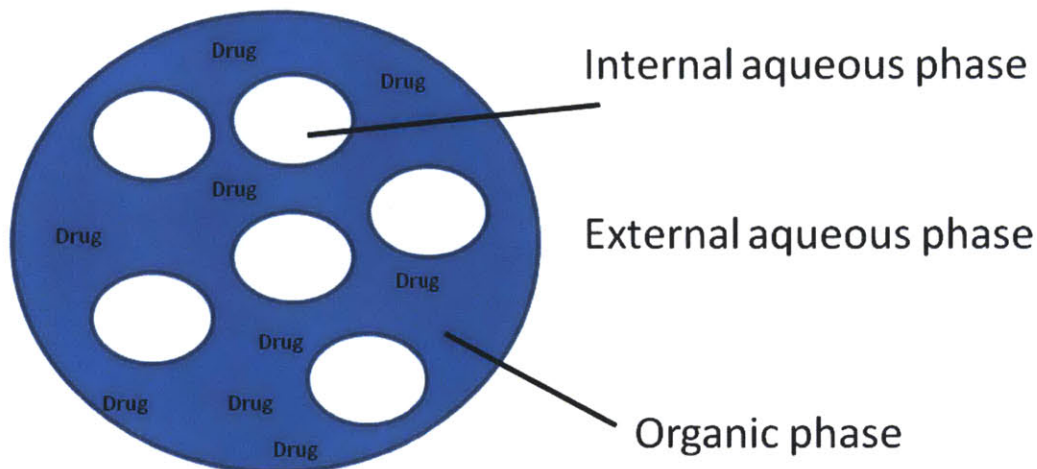


Figure 6: Microparticles with drug loaded in the organic phase

The double emulsion allows flexibility for drugs of different polarity to be loaded into the microparticle. Due to the low solubility of Saquinavir in aqueous solutions, Saquinavir was loaded into the organic phase. Although the additional step of the addition of the internal aqueous phase is unnecessary, it was kept to demonstrate the flexibility of the double emulsion synthesis as well as to be consistent with the microparticle syntheses for the aqueous soluble drugs. Three different syntheses were performed, each with a different concentration of Saquinavir in the organic phase.

### *1. Organic phase preparation*

Briefly, 50 mg of Saquinavir was dissolved in 1.5625 mL of DMSO for a concentration of 32 mg/mL. Next 80 mg of poly(lactic acid-*co*-glycolic acid) (PLGA) from Lakeshore Biomaterials 50:50 DLG 4A (inherent viscosity 0.35-0.45 dL/g) was dissolved in 5 mL of a mix of dichloromethane (DCM) and the DMSO+Saquinavir solution in a 10 mL glass vial. Three different loadings, defined as the ratio of Saquinavir to PLGA were used to examine the effects of different loadings. A 20% loading solution was made by adding the 80 mg of PLGA to 0.5 mL of DMSO+Saquinavir and 4.5 mL of DCM. A 10% loading solution was made by adding the 80 mg of PLGA to 0.25 mL of DMSO+Saquinavir and 4.75 mL of DCM. Finally, a 1% loading solution was made by adding the 80 mg of PLGA to 25  $\mu$ L of DMSO+Saquinavir to 4.975 mL of DCM. Each solution was shaken for at least 30 minutes to ensure complete dissolution of PLGA in solution.

## *2. Aqueous phase preparations*

The internal aqueous phase used was simply PBS. The external aqueous phase used was a 0.5wt% poly(vinyl alcohol) (PVA) solution from MPBiomedicals catalog #151937, with a molecular weight of 15000. 40 mL of PVA was prepared in a 50 mL Erlenmeyer flask.

## *3. Particle preparation and work-up*

These steps to the particle preparation are outlined above in **Figure 5** above. Synthesis was performed in a fume hood due to the volatile organic solvents. A MISONIX ultrasonic liquid processor XL-2000 Series sonicator was set to 7 Watts and cleaned alternating with DCM and acetone for 30 seconds in a 20 mL glass vial, ending with DCM and drying with a Kimwipe. The same was done for an IKA T25 Digital Ultra-Turrax homogenizer, which was set at 16,000 RPM. The organic phase, which was approximately 5 mL of solution in a 10 mL glass vial, was

placed in an ice bath and sonicated for 30 seconds with 500  $\mu$ L of the internal aqueous phase, PBS, introduced with a micropipette immediately with the beginning of the sonication by dripping down the sonicator probe tip. While sonicating, the sonicator tip was moved up and down a number of times and left close to the bottom of the tip to fully emulsify the two solutions. After 30 seconds, the sonicator was turned off and 10 mL glass vial of the emulsified internal aqueous phase and organic phase was replaced with the Erlenmeyer flask containing the 40 mL of external aqueous phase. The homogenizer was placed into the external aqueous flask on ice and the first emulsion was added by glass pipette again down the homogenizer, but as far into the solution as possible. The homogenization step lasted 3 minutes, including the approximately 30 seconds to introduce the first emulsion into the second emulsion. After the homogenization, the flask was stirred overnight in the fume hood to evaporate to remove excess solvent. The first emulsion created nanoparticles of the internal aqueous phase in the organic phase. The second emulsion created microparticles of the first emulsion in the external aqueous phase.

After one day, the particle suspensions were then aliquotted into 15 mL conical tubes and centrifuged at 3000 RPM for 10 minutes. The supernatant was removed and the suspensions were washed once: ~13 mL of Milli-Q (MQ) water was added to each tube, the tubes were vortexed, centrifuged, and the supernatant was again removed. The suspensions were then resuspended in 1 mL of MQ water. 200  $\mu$ L of the suspension was aliquotted into Eppendorf tubes, usually around 5 to 6 tubes, with the excess kept for particle characterization. These suspensions were lyophilized to store them. The aliquots were flash frozen in liquid nitrogen and then perforations were made in the top of the tube before they were placed in vacuum. After a few days, the lyophilized particle suspensions were then stored in 50 mL conical tubes with DRIER dessicant and placed in the 4 degree Celsius refrigerator.

#### 4. *Particle Characterization*

The particles were then characterized to determine size, zeta potential, concentration, and yield. To determine concentration and yield, the total excess suspension after storing 200 mL aliquots was measured to determine the total volume of particle suspension. PCR Eppendorf tubes were weighed and then aliquots of 25  $\mu\text{L}$  were put in each tube and lyophilized in the same lyophilization process to store the suspensions. After a few days, these Eppendorf tubes were weighed and the difference was used to calculate the concentration of the particle suspension. The microparticle size and zeta potential were determined using a BIC 90+ Particle Analyzer, a dynamic light scattering (DLS). Polystyrene disposable cuvettes were used and filled to the 10 mm mark with MQ water. 30  $\mu\text{L}$  of the particle suspension was then added. The software was used to select “uniform spheres” and “liquid” as the type of particles to detect and the base liquid, respectively. The particle analyzer was run and determined the particle size and polydispersity. The zeta potential, which is a surface charge measurement that can indicate stability of colloidal dispersions, was determined in a similar manner. The same diluted solution of microparticles was pipetted into the rinsed cuvette and the rinsed electrode was placed into the cuvette with solution. Sufficient solution was added so that the solution covered both electrode plates. The software was used to enter the size of the particles from the previous step, as well as set the base liquid to water and the pH to 5.00.

#### iv. Microparticle loading

To determine the amount of drug that was successful loaded into the microparticles, a lyophilized aliquot of microparticles with known mass was hydrolyzed for one day with 0.2 M NaOH. The control microparticles were also hydrolyzed under the same conditions as the Saquinavir microparticles and were used as the base reading. This was to eliminate any

interference from signal from PLGA. The solutions were then diluted into the range of the linear portion of the standard curve and the absorption was determined from the UV visible spectrophotometer. The linear regression from the standard curve was then used to calculate the loading.

v. Microneedle synthesis and characterization

The microneedle synthesis from beginning to end is a multi-step process that requires the use of a number of intermediate processes to create the final drug loaded microneedle arrays. Figure 7 below outlines the entire process.

PDMS Mold Fabrication

MN Synthesis from PDMS Mold

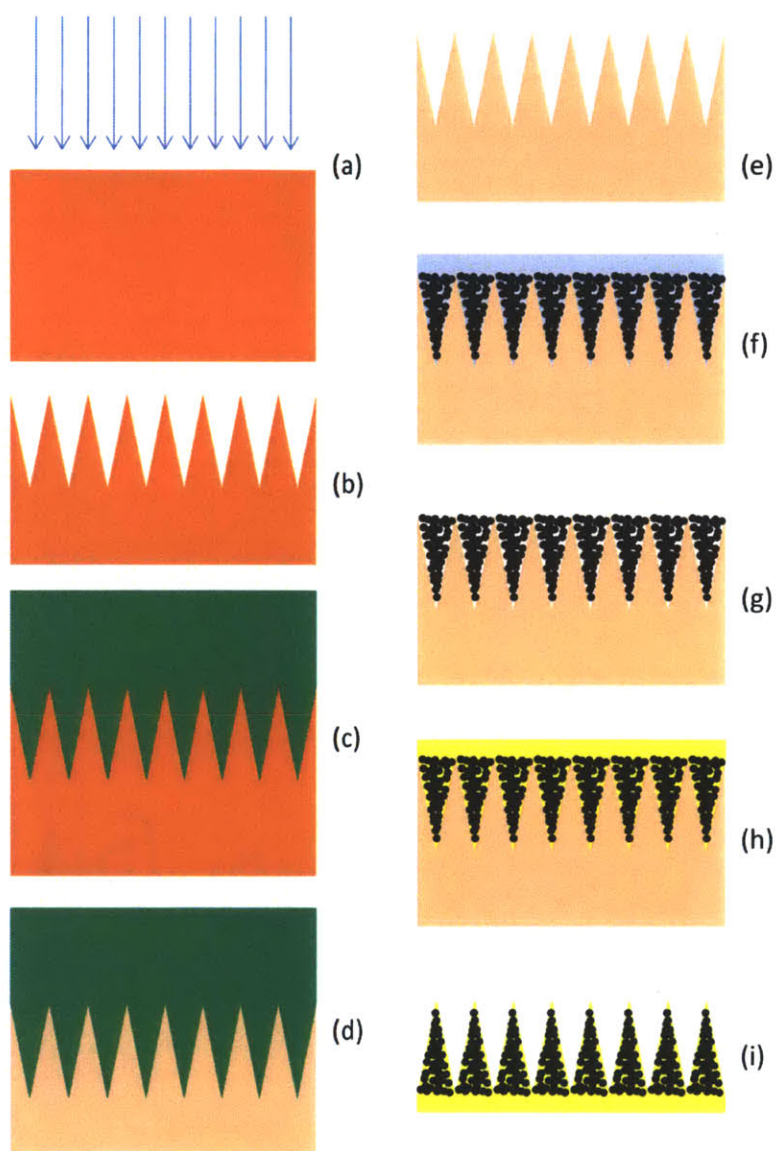


Figure 7: Outline of the microneedle fabrication process. (a) Master molds were generated from solid PDMS blocks through laser ablation micro machining of the surface to create the mold cavities (b) The master molds (c) These master molds were then used to cast PLLA MN arrays (d) These PLLA MN arrays were used to cure PDMS replicate molds (e) The PDMS replicate molds were used to create the drug loaded MN arrays (f) The drug, in the form of microcrystals or microparticles, was deposited onto the molds and centrifuged into the cavities (g) The solution dried leaving just the microcrystals or microparticles (h) PAA was then deposited and centrifuged and allowed to dry to create a solid matrix (i) The microneedles were then removed from the mold and ready to use.



### *1. PDMS microneedle mold fabrication*

With the particles synthesized, microneedles were then synthesized using polydimethylsiloxane (PDMS) molds, shown in **Figure 8** below. The PDMS mold fabrication refers to steps (a-e) in **Figure 7** above. These PDMS molds were synthesized from poly-L-lactide (PLLA) microneedles, which were created from master PLLA microneedles that were created from PDMS master molds, created from laser ablation. The microneedles were mounted in silicon isolators on the bottom of a culture dish and PDMS precursor and curing agent in a 10:1 ratio (3.8mg curing agent + 34.2 mg PDMS precursor) was mixed well and added. It was cured at 65C for five hours and then the MNs were removed from the PDMS mold, which was then sonicated in a jar filled with acetone for 60 minutes. The mold was finally incubated in a vacuum oven overnight at 140C and finally placed in the freezer for 30 minutes before being ready to be used.



Figure 8: PDMS mold used to synthesize microneedles

## 2. *Microparticle deposition*

Both the control microparticles and Saquinavir microparticles were encapsulated in the microneedles in essentially the same process. Only the highest concentration of the microparticles was used to maximize the potential loading in the microneedles. 140  $\mu\text{L}$  of MQ water was deposited into each array well of the PDMS mold and the mold was placed in a vacuum chamber. The microparticle deposition refers to steps (f-g) of **Figure 7** above. Vacuum was applied carefully a few times for 5-10 seconds in order to remove air bubbles. The addition of this water is to remove air and allow for the deposition of the particles into the cavities. 70  $\mu\text{L}$  of the water was removed from each well and replaced with 70  $\mu\text{L}$  of microparticle suspension

with a concentration of .0285 mg/ $\mu$ L. Both the control “empty” microparticles and the 20% loaded microparticles aliquots had extremely similar masses of approximately 10.94 mg. This corresponded to dissolving each aliquot in 383  $\mu$ L of water and adding 70  $\mu$ L of solution to each array well. The molds were centrifuged at 1850 RPM for 15 minutes. The supernatant was removed and the molds were left to dry on the bench top for an hour.

### *3. Polyacrylic acid addition*

This final step refers to steps (h-i) in **Figure 7** above. Following the deposition of the microparticles, PAA at 35% concentration by weight was added to help the microneedles maintain their shape and help drive the delivery of the particles. To add the PAA, 2 mm adhesive silicon isolators were placed on top of the mold and approximately 300  $\mu$ L of PAA was added to each well to the brim of the adhesive silicon isolator. The molds were then centrifuged at 1850 RPM for 25 minutes. The molds were then left to dry on the bench for 48 hours before they were placed in the dessicator for an additional 48 hours. The microneedles were removed by placing the molds in the -20C freezer for 30 minutes and using tweezers to pull them out. They were then stored in the dessicator until use.

### *4. Microneedle characterization*

Microneedles were imaged using an optical microscope to check dimensions of the microneedles as well as viewing the separation of particles and PAA. A Leitz DMRX optical microscope with a Nikon DXM1200F Digital Camera was used.

#### vi. Microneedle loading

At first, each microneedle array was placed in an Eppendorf tube and 1.5 mL of 0.2 M NaOH was added so that the microneedle array was fully submerged. After one day, the entire

microneedle array had hydrolyzed. This method, however, proved impossible due to the absorbance of PAA.

Instead, each microneedle array was vortexed in 1.5 mL of MQ water for 60 seconds so only the contents of the tips would be released from the microneedles. The Eppendorf tube was then centrifuged and the supernatant was removed. The contents of the tips were then hydrolyzed in 0.5mL of 0.2 M NaOH and after a day, the absorbance of the solution was detected using the UV visible spectrophotometer. The intensity corresponded to the loading concentration from the standard curve.

### **c. Results and discussion**

#### **i. Standard curves**

Saquinavir had a peak absorption at 238 nm and showed a linear optical absorption at this wavelength over a concentration range from 2.5  $\mu\text{g/mL}$  to 10  $\mu\text{g/mL}$ , as shown in **Figure 9**, below. This corresponded to the upper range of the literature value, which was linear from 2.5 ng/mL to 25  $\mu\text{g/mL}$ <sup>26</sup>. The standard curve was tested on three different occasions, all plotted below. The variation from the third could be due to a variety of factors, including contamination from the cuvette.

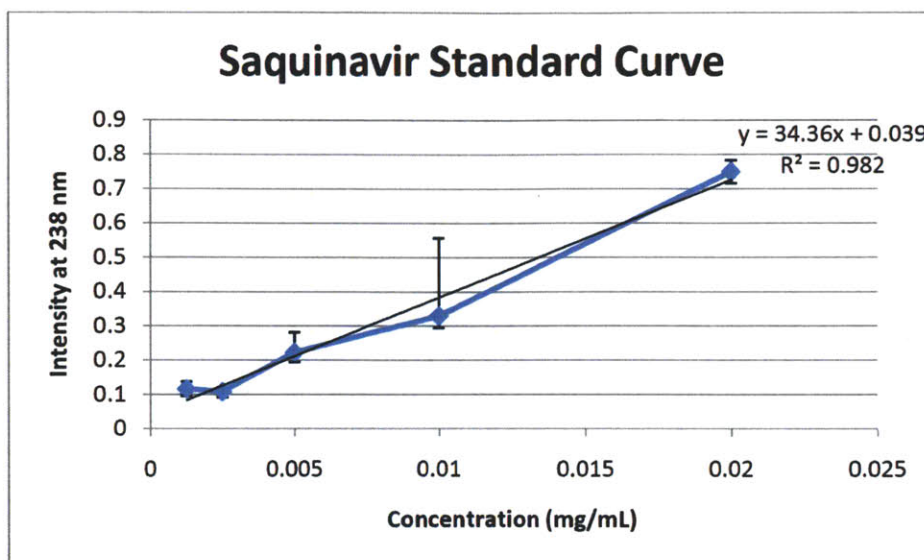


Figure 9: Saquinavir Standard Curve for with error bars from 3 series of measurements

In addition, the 238 nm peak absorption matched reported absorption values from literature, as is apparent in **Figure 10** below.

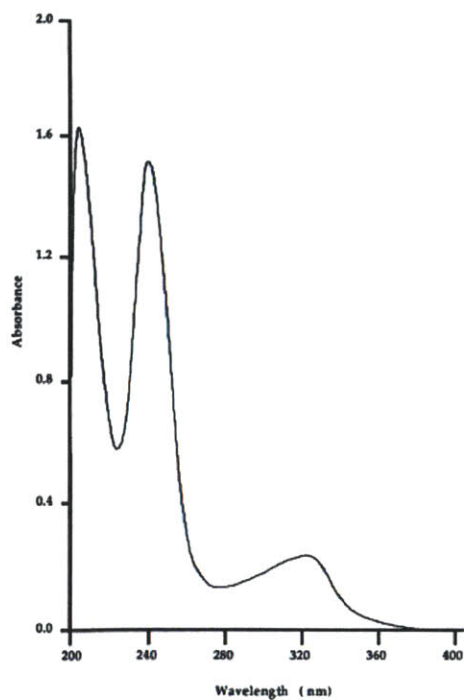


Figure 10: From Ha et al, the UV-spectrum of Saquinavir-mesylate dissolved in .01M HCl<sup>25</sup>

The peak for the Maraviroc dilutions was at 257 nm and was linear and detectable from concentration 0.3125 mg/mL to 0.1 mg/mL. **Figure 11**, below, shows the calculated standard curve from these readings. There was a large difference, however, between this data and literature data. The literature values for the peaks of absorption were 197 nm and 300 nm and linear up to 2500 ng/mL. There could be a number of explanations for this discrepancy, including the limitations of the spectrophotometer to only measure down to 200 nm, but more likely because the structure has a degree of conjugation that is lower than the threshold needed to detect a signal with the spectrophotometer. Because of this discrepancy, it was decided not to continue with Maraviroc because of the uncertainty in determining Maraviroc concentration and therefore loading of microparticles and microneedles that were loaded with Maraviroc.

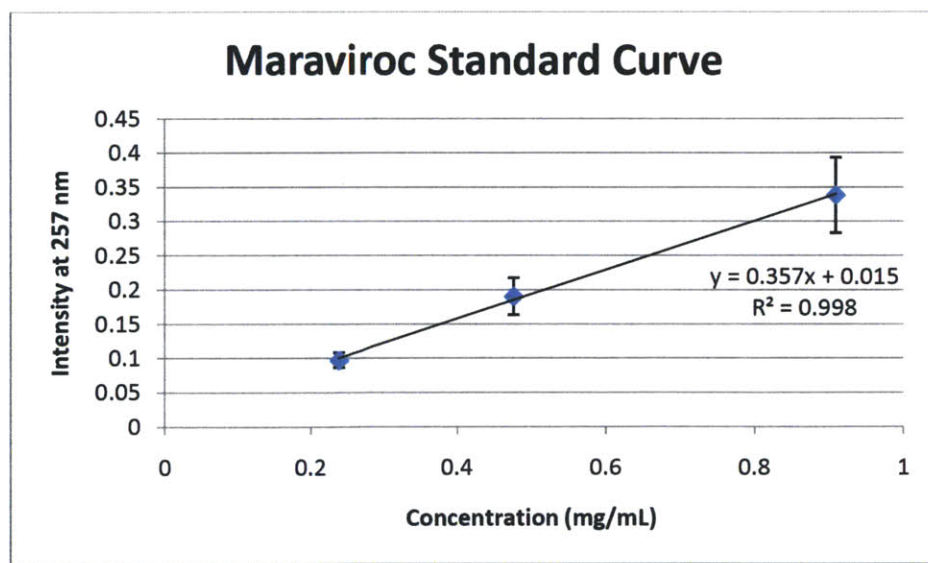


Figure 11: Maraviroc standard curve at 257 nm zeroed with .2M NaOH + varying levels of DMSO to match the concentration present in Maraviroc samples. Error bars derived from replicate measurement zeroed only in 0.2M NaOH.

ii. Microparticles

The drug-loaded PLGA microparticles were characterized to understand their properties and hypothesize about how they will act for their intended use and to understand the double emulsion synthesis. The size, polydispersity, and zeta potential all give insight into how the particles might dissolve and interact within the body and the yield of the particles indicates how effective the double emulsion synthesis is in yielding particles. **Table 2** shows the results from the Saquinavir microparticles and the results from the control particles. Both groups of microparticles had expected properties with no anomalies.

<i>Microparticles</i>	<i>Hydrodynamic Diameter (nm)</i>	<i>S.E.</i>	<i>PDI (polydispersity)</i>	<i>S.E.</i>	<i>Zeta potential (mV)</i>	<i>S.E.</i>	<i>Yield: recovered mass of particles (%)</i>	<i>Mass of particles per 200uL lyophilized aliquot (mg)</i>
PLGA + Saquinavir (20%) (0.5% PVA)	1134.7	29.2	0.061	0.038	-38.51	0.15	75.17%	10.93
PLGA + Saquinavir (10%) (0.5% PVA)	1112.2	84.7	0.073	0.042	-38.21	0.09	93.50%	13.60
PLGA + Saquinavir (5%) (0.5% PVA)	1027.2	20.1	0.064	0.039	-38.08	0.12	77.00%	11.20

<i>Microparticles</i>	<i>Hydrodynamic Diameter (nm)</i>	<i>S.E.</i>	<i>PDI (polydispersity)</i>	<i>S.E.</i>	<i>Zeta potential (mV)</i>	<i>S.E.</i>	<i>Yield: recovered mass of particles (%)</i>	<i>Mass per 200uL lyophilized aliquot (mg)</i>
PLGA + DMSO, DCM (20%) (0.5% PVA)	1205.8	91.3	0.005	0.000	-42.64	1.55	75.17%	10.93
PLGA + DMSO, DCM (10%) (0.5% PVA)	1727.1	122.3	0.038	0.033	-28.67	1.43	78.83%	11.47
PLGA + DMSO, DCM (1%) (0.5% PVA)	2229.3	157.9	0.141	0.067	-35.23	2.33	64.17%	9.33

Table 2: Characterization results for Saquinavir loaded particles, above, and the control particles, below.

iii. Microparticle loading

The hydrolyzed microparticles showed higher concentrations of Saquinavir with an increase in the Saquinavir loading. **Table 3** below shows a regression between the loading of the particles and the actual ratio as determined by the absorbance signal and **Figure 12** shows the correlation graphically with a linear fit.

<i>Loading (Saquinavir:PLGA)</i>	<i>Actual loading (mass of Saquinavir per mass of particles)</i>
----------------------------------	--



20%	1.35%
10%	0.98%
1%	0.42%

Table 3: The correlation between loading ratio during synthesis and actual loading of microparticles.

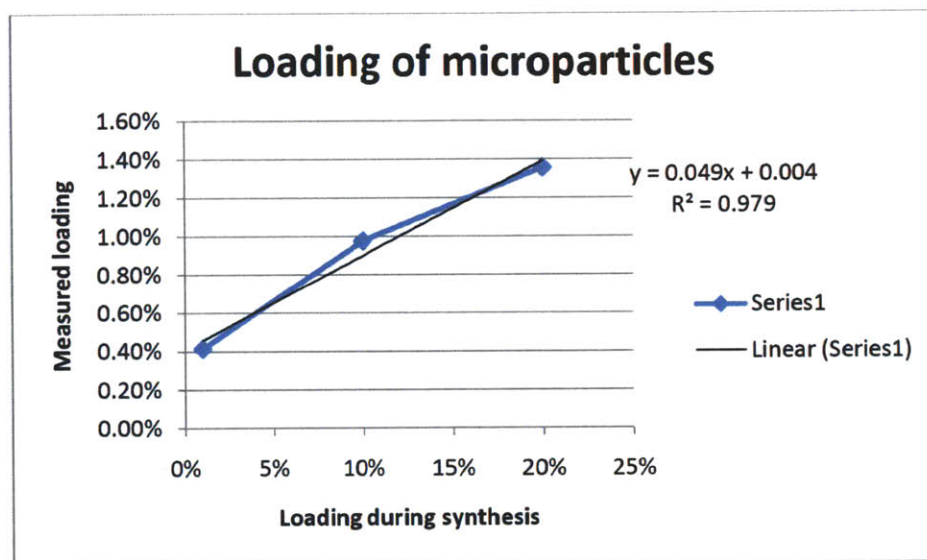


Figure 12: Correlation shown graphically and approximated as linear between increase in loading during synthesis and actual loading. No error analysis available due to absence of replication measurements.

iv. Microneedles

Below, in **Figure 13**, are images that were taken of the microneedles. The tips are a different color than the rest of the microneedle due to the microparticles. The rest of the microneedle is PAA.

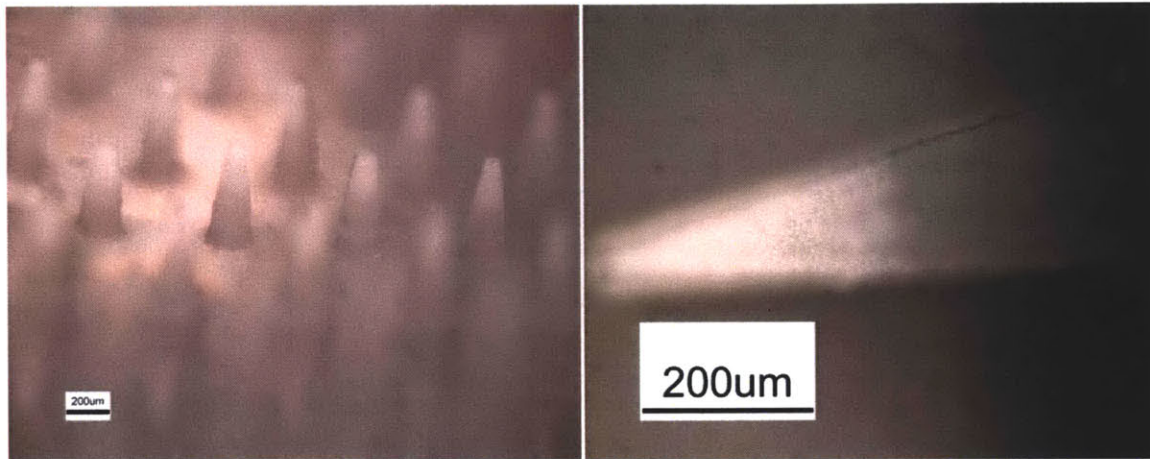


Figure 13: On the left, the Saquinavir microparticle loaded microneedles and on the right, a higher magnification image of a control microparticle loaded microneedle.

v. Microneedle loading

The absorbance of the microneedle contents hydrolyzed with 0.2 M NaOH overnight, with a zero base line of the microneedle contents of the microneedles synthesized with the control particles, showed a strong peak at 240 nm and a small peak at 219 nm, which most likely correspond to the difference in PLGA between the Saquinavir particles and the control particles.

The microneedles with the 20% loaded Saquinavir showed a loading consistent with expected results. The 0.899 intensity corresponds to a concentration of .0239 mg/mL. The microneedle contents were dissolved in 0.5 mL of 0.2 M NaOH, which would correspond to .0120 mg of Saquinavir per array. With a 20% Saquinavir microparticle loading of 1.35% determined from the microparticle loading experiment, this would correspond to 883 µg of particles per microneedle array. Based on the volume of approximately 1 mg per array calculated previously, this would match the prediction.

Other studies have examined how drugs introduced with microneedles were able to reach systemic circulation. One such study showed the plasma free insulin levels, after a microneedle

injection of 15 units of insulin (approximate total of 682.5  $\mu\text{g}$  of insulin), reached a peak of over 100 microU/mL (4.55 ng/mL)<sup>31</sup>. For 12  $\mu\text{g}$  of Saquinavir per array, this would translate to 0.08 ng/mL, well below the minimum effective concentration of 100 ng/mL required for Saquinavir. Because of this factor of 1250, an idea to use drug crystals to maximize the loading of an array close to the 1 mg limit came about. The use of drug crystals, combined with the using multiple arrays, could increase the amount of drug delivered to the necessary levels. Further, the absorption kinetics of Saquinavir could be quite different than that of insulin. In addition, Saquinavir, unlike insulin, is most effective in the lymphatic system and might have higher concentration levels in the local lymphatic system.

#### **d. Conclusion**

It has been shown that the antiretroviral drug, Saquinavir, can be loaded effectively into microparticles and that these microparticles can then be loaded in microneedles. It remains unclear whether the loading is sufficient to completely replace current delivery for Saquinavir, however these preliminary results are promising. Microneedle deliveries could supplement current delivery in order to specifically target viral reservoirs.

### **III. Microneedle Delivery of Antibiotics**

#### **a. Introduction**

Antibiotics are of particular interest due to the prevalence of bacterial infections and because of the potential for increase in efficacy of these drugs from the delivery of the antibiotics directly to the lymphatic system. Antibiotics are currently delivered in three main forms: orally and topically for the majority of infections that are usually localized and intravenously for more serious, usually systemic infections. One specific application for the microneedle delivery of antibiotics would be in battlefield situations, where open wounds and battlefield trauma lead to high risk of infection. The lack of sterile conditions on the battlefield and the delay in being able to evacuate the casualty both contribute to the need of effective antibiotics. The casualty is usually treated intravenously with an antibiotic in order to immediately treat the infection<sup>32</sup>. Microneedle application could be as efficacious, while eliminating the need for trained medical personnel to set up the IV as well as enabling the casualty to self-apply the antibiotic immediately. Typical IV dosages are actually similar to the oral pill dosages; IV dosages are only approximately 20% less<sup>35</sup>. Therefore, the use of microneedle delivery of antibiotics to replace IV introduction of drug would carry the same benefits of replacing high oral pill dosage and frequent dosage.

This specific application was kept in mind when a candidate drug was selected to test the feasibility of this idea. In addition, as with the antiretroviral drugs, bioavailability, half-life, and total dosage were all factors in the drug choice.

#### **b. Materials and Methods**

i. Drug Choice

The drug chosen was Ciprofloxacin based on its desired characteristics, shown below in **Table 4**. In addition, Ciprofloxacin is a commonly administered drug on the battlefield for a variety of injuries<sup>32</sup>. Ciprofloxacin, which has the structure shown below in **Figure 14**, was obtained from Sigma Aldrich. It is a second generation fluoroquinolone that targets the bacteria's ability to rewind its DNA during DNA synthesis.

<i>Drug name</i>	<i>Bioavailability</i>	<i>Percent reach Circulation</i>	<i>Half-life (hours)</i>	<i>Dose frequency (doses/day)</i>	<i>Total Daily Dosage (mg)</i>	<i>Minimum inhibitory concentration</i>
Ciprofloxacin	70%, .5 to 5% <sup>37,38</sup>	~10% <sup>37</sup>	4 <sup>35</sup>	2 <sup>32</sup>	800 <sup>32</sup>	<1µg/mL, .062- 32µg/mL <sup>33,34</sup>

Table 4: Drug properties for Ciprofloxacin that were used to select it as a candidate drug

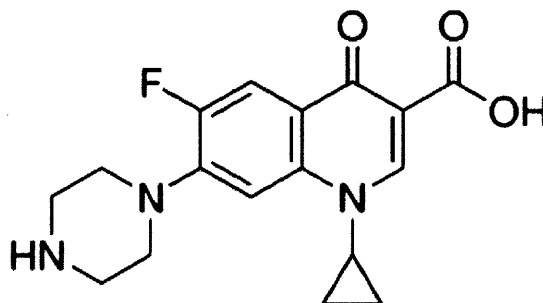


Figure 14: The structure of Ciprofloxacin, obtained from Sigma Aldrich.<sup>36</sup>

ii. Standard curves

As with Saquinavir, standard curves were created in order to determine the concentration of Ciprofloxacin in solution. Samples were created with known concentration, diluted, and then the absorbance was measured with a UV-visible spectrophotometer. The measurements were recorded to create a standard curve.

Ciprofloxacin is soluble up to 30 mg/mL in pH 3 solution<sup>38</sup>. Three different concentrations were initially made of 30 mg/mL, 10 mg/mL and 5 mg/mL. The corresponding amount of ciprofloxacin was put in 20 mL of water and then drops of 2.4 N hydrochloric acid (HCl) were added until the Ciprofloxacin dissolved in solution. The amount of 2.4 N HCl added was inconsequential compared to the volume of the initial solution. The same glass cuvette used for the Saquinavir and Maraviroc curve was used for the readings with the UV spectrophotometer, which did a quick read from 200 nm to 450 nm. The 5 mg/mL solution was used to initially create the standard curve and was then tested with dilutions from the other two solutions. In addition, dilutions in 0.2M NaOH were also created at 17  $\mu\text{g/mL}$  and 5  $\mu\text{g/mL}$  to ensure similar absorbance values since loadings were going to be read in 0.2 M NaOH.

iii. Microparticle synthesis

The microparticle synthesis to encapsulate the ciprofloxacin was the same double emulsion synthesis as for the Saquinavir; however, the drug ciprofloxacin was encapsulated in the internal aqueous phase as opposed to the organic phase. **Figure 15** below shows the structure of the microparticle.

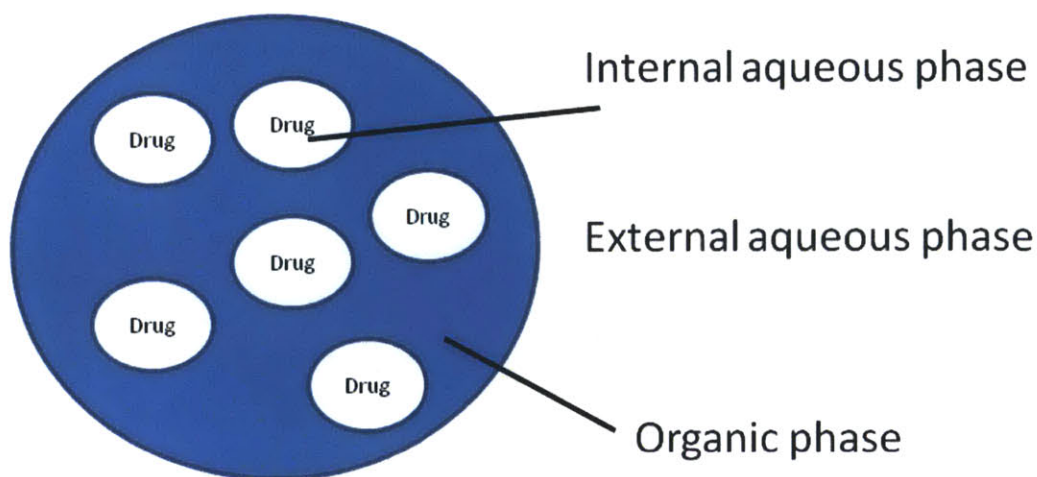


Figure 15: Microparticles with drug loaded in the internal aqueous phase

Three syntheses were done for three different concentrations of Ciprofloxacin, 30 mg/mL, 10 mg/mL, and 5 mg/mL.

1. *Organic phase preparation*

For each synthesis, 80 mg of poly(lactic-co-glycolic) acid (PLGA) from Lakeshore Biomaterials 5050 DLG 4A (inherent viscosity 0.35-0.45 dL/g) was dissolved in 5 mL of dichloromethane (DCM). Each solution was shaken for at least 30 minutes for complete dissolution of PLGA.

2. *Aqueous phase preparations*

The internal aqueous phase was simply the 30 mg/mL, 10 mg/mL, and 5 mg/mL solutions of Ciprofloxacin dissolved in water and 2.4 N hydrochloric acid to create a solution of approximately pH 2. The external aqueous phase used was 40 mL of .5% poly(vinyl alcohol) (PVA) solution from MPBiomedicals catalog #151937 with a molecular weight of 15000 that was prepared in a 50 mL Erlenmeyer flask.

3. *Particle preparation and work-up*

Particle preparation and work-up was carried out as described in Chapter II, Section b.iii.3., but with 500  $\mu$ L of the internal aqueous phase being solutions of ciprofloxacin and the 5 mL of the organic phase being PLGA in DCM.

4. *Particle characterization*

Particle characterization was carried out as described in Chapter II, Section b.iii.4.

iv. Microparticle loading

Microparticle loading was carried out as described in Chapter II, Section b.iv.

v. Microcrystals

In addition to the testing of microneedle loading of microparticles, the test of microneedle loading of microcrystal was also of interest. Microcrystals are simply pure crystalline drug with sizes on the micron scale. This would allow for much higher loading of microneedles with drug, although the controlled release properties might be significantly affected. There were two main approaches to synthesizing the microcrystals: precipitate the crystals out of dissolved solution and sonicate the ciprofloxacin in water.

The precipitation method involved first dissolving the ciprofloxacin in pH 2 solution of water and 2.4 N HCl and then the addition of 0.2M NaOH until the ciprofloxacin precipitated out of solution. This was done for the 30 mg/mL solution for three different pH change rates. One was 1 mL of 0.2M NaOH every five seconds, the second was 300  $\mu$ L of NaOH every 10 seconds, and the last was 500  $\mu$ l of 0.2M NaOH every 10 seconds.

The sonication in water method involved creating concentrations of Ciprofloxacin in water and then sonicating each concentration for one minute at 7 Watts.

The microcrystal solution from each synthesis was then characterized using DLS, dynamic light scattering, on a Brookhaven 90Plus instrument.

vi. Microneedle synthesis and characterization

Microneedle synthesis and characterization carried out as described in Chapter II, Section b.v.

vii. Microneedle loading

Microneedle loading carried out as described in Chapter II, Section b.iv.



## c. Results and discussion

### i. Standard curve

The ciprofloxacin had a peak absorption at around 270 nm and was linear from 1.25-25  $\mu\text{g}/\text{mL}$ , which matched literature values of a peak absorption at 271.4 nm and linear from 2-10  $\mu\text{g}/\text{mL}$ <sup>35</sup>. The standard curve is plotted below in **Figure 16**. The dilutions from all three concentrations as well as the dilutions of ciprofloxacin in 0.2M NaOH were all well correlated, indicating strong confidence in determining the concentration of ciprofloxacin from absorbance spectrum.

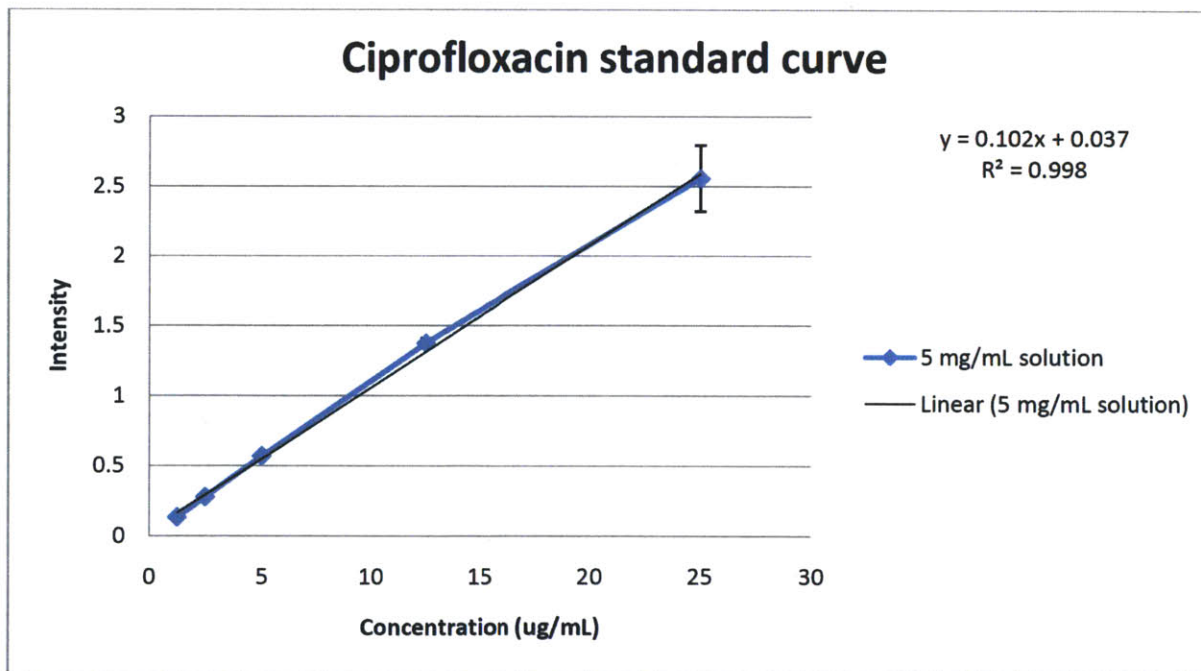


Figure 16: Ciprofloxacin standard curve, checked with multiple dilutions at different pH as well as solution in 0.2M NaOH. Error bars derived from replicate measurements of different starting concentrations (10 mg/mL and 30 mg/mL)

### ii. Microparticles

The same properties for the Saquinavir microparticles were determined for the ciprofloxacin microparticles in order to fully understand the ciprofloxacin microparticles. Table 5 below shows these properties, which are all expected. Only the yield and total mass per 200  $\mu$ L aliquot are lower than expected. This is most likely due to the fact that the extra step required to encapsulate the drug in the internal aqueous phase and subsequent encapsulation in the organic phase could lead to significant loss of both the drug in the internal aqueous phase as well as a loss in volume of the aqueous phase which does not become encapsulated and is washed away.

<i>Microparticles</i>	<i>Hydrodynamic Diameter (nm)</i>	<i>S.E.</i>	<i>PDI (polydispersity)</i>	<i>S.E.</i>	<i>Zeta potential (mV)</i>	<i>S.E.</i>	<i>Yield: mass of particles recovered (%)</i>	<i>Mass per 200 <math>\mu</math>L lyophilized aliquot (mg)</i>
PLGA + CIPRO (5mg/mL) (0.5% PVA)	1610.6	71.1	0.149	0.060	-17.18	4.03	36.67%	5.33
PLGA + CIPRO (10mg/mL) (0.5% PVA)	1500.8	60.2	0.022	0.017	-22.44	3.38	47.67%	6.93
PLGA + CIPRO (30mg/mL) (0.5% PVA)	1681.3	127	0.036	0.031	-31.48	1.62	27.50%	4

Table 5: Characterization of ciprofloxacin loaded microparticles with different loading levels

iii. Microparticle loading

Only the two highest concentrations of ciprofloxacin were encapsulated in the microparticles. The higher concentration encapsulation showed a higher signal after hydrolysis of the microparticles. There was also a significant loss during encapsulation of ciprofloxacin for reasons cited earlier. **Table 6**, below, shows the different predicted loading and actual loading for three different concentrations of ciprofloxacin used in the internal aqueous phase.

<i>Concentration of internal aqueous phase</i>	<i>Loading (Ciprofloxacin:PLGA+ Ciprofloxacin)</i>	<i>Actual loading of particles (mass of ciprofloxacin: mass of particles)</i>
30 mg/mL	0.158	0.00197
10 mg/mL	0.0588	0.000513

Table 6: Different predicted and actual loadings for different concentrations of Ciprofloxacin in the internal aqueous phase

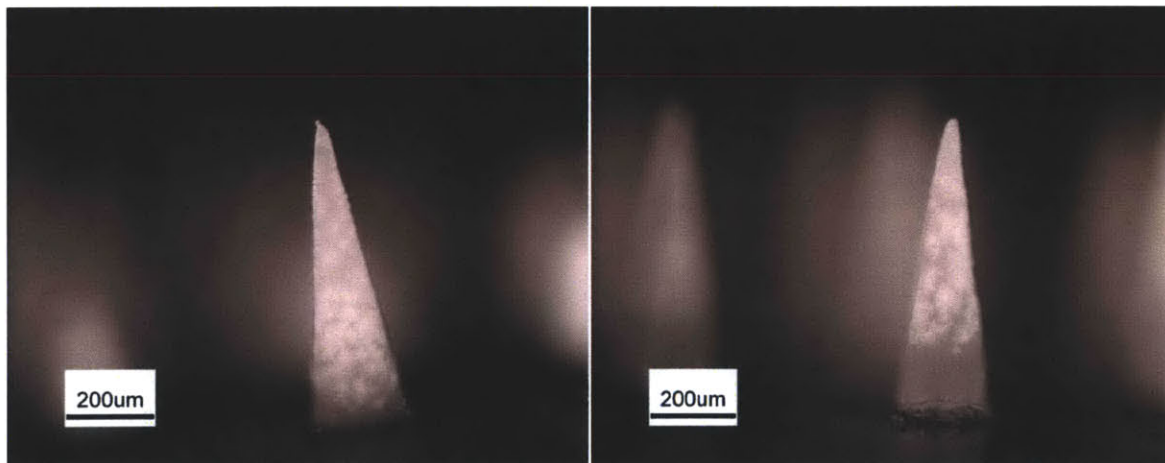
iv. Microcrystals

The size of the microcrystals seemed highly dependent on concentration. There was a large distribution of sizes ranging from a few hundred nanometers to tens of microns. The majority of distribution, however, was between 1 and 10 microns. The precipitated method seemed to cause a more uniform distribution.

The sonicated microcrystals used in the microneedles had a measured concentration of .0077 mg/ $\mu$ L, which translated to a maximum of 537  $\mu$ g in each microneedle array. The precipitated microcrystals had a hypothetical maximum concentration of .03 mg/  $\mu$ L, which would translate to a promising 2.1 mg per microneedle array. In actuality, it was slightly lower due to dilution from the HCl and NaOH. There was not a significant affect from altering pH or altering pH change on the size of the microcrystals.

v. Microneedles

The images below, **Figure 17**, show the microneedles from two loadings of the ciprofloxacin microparticles and the two different microcrystal syntheses. The two images of the ciprofloxacin microparticle loaded microneedles have a difference in coloration due to the loading of the microparticles. The microneedles loaded with the ciprofloxacin microcrystals, however, show no difference in coloration due to the acidity of the PAA dissolving the microcrystals. This phenomenon could have a very interesting effect when introduced into the more basic plasma or blood solution in the human body, where it would then crystallize depending on the concentration. Because of the low concentration, it might in fact stay dissolved and not recrystallize. These are questions that remain to be answered.



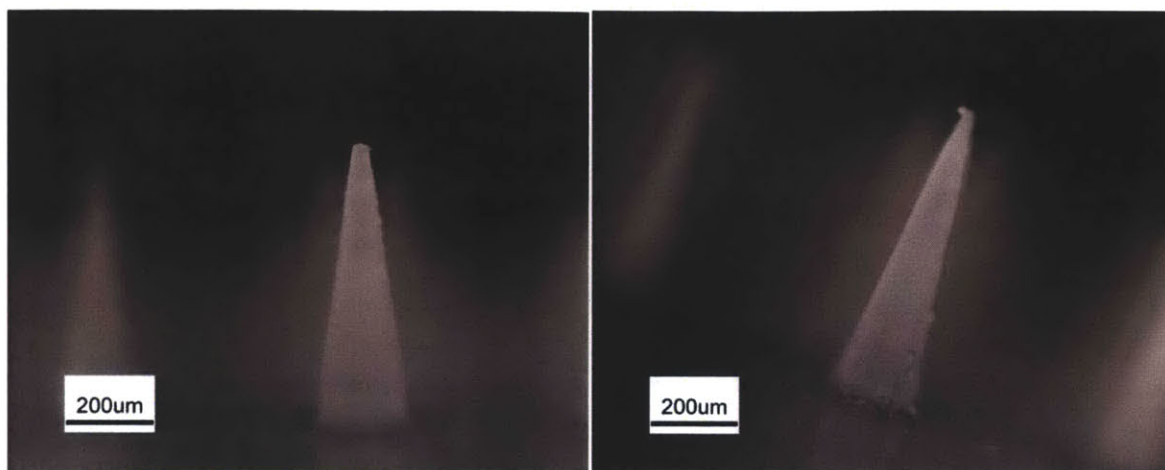


Figure 17: From top left to right: 30 mg/mL Cipro MP MN, 10 mg/mL Cipro MP MN; bottom left to right: sonicated ciprofloxacin microcrystal MN, precipitated ciprofloxacin microcrystal MN

vi. Microneedle loading

The microneedles loaded with the ciprofloxacin microparticles demonstrated a signal corresponding to .41  $\mu\text{g}$  of ciprofloxacin per array for the 30 mg/mL concentration of ciprofloxacin in the microparticles and 0.177  $\mu\text{g}$  of ciprofloxacin per array for the 10 mg/mL concentration of ciprofloxacin in the microparticles. Based on the ciprofloxacin loading in microparticles for these two concentrations, this would indicate 208  $\mu\text{g}$  of microparticles and 345  $\mu\text{g}$  of microparticles in the 30 mg/mL and 10 mg/mL ciprofloxacin microneedle arrays, respectively. These numbers are a factor of 2 to 3 lower than the calculating loading capacity of approximately 1mg for each microneedle array. One factor that could contribute to this is that much of the microparticles are centrifuged between the microneedles as opposed to into the microneedles.

The microneedle arrays loaded with the sonicated microcrystals led to a loading of 1.7  $\mu\text{g}$  of ciprofloxacin per array. The arrays with the precipitated microcrystals led to a loading of 165  $\mu\text{g}$  of ciprofloxacin per array. The sonicated microcrystals loaded microneedles produced a

loading much lower than expected, but the precipitated microcrystals loaded microneedles showed promise, although they were still an order of magnitude lower than expected. Based on the calculated concentrations, a maximum of 175  $\mu\text{g}$  and 2.1 mg of microcrystals for the precipitated and sonicated microcrystals should have been expected, respectively. A reason for this discrepancy could be that because of the varied size distribution for both microcrystals, but particularly the sonicated microcrystals, the larger crystals could have blocked the other sizes from centrifuging down into the microneedles. In addition, the smaller sizes of less than 1 micron would not centrifuge down and would be washed away. Finally, much could have been centrifuged in between the microneedles, which would have been washed away before the PAA addition, instead of into the microneedles.

Using the analogous insulin analysis, the 165  $\mu\text{g}$  from the precipitated Ciprofloxacin microcrystals would translate to 1.1 ng/mL. This is well below to approximately 1  $\mu\text{g/mL}$  needed for a minimum inhibitory concentration. If the entirety of the 1 mg was loaded using the microcrystals, however, this would lead to 6.67 ng/mL, still too low to cover the highest required concentration of antibiotics. Some strains of bacteria, however, require .062  $\mu\text{g/mL}$ , meaning the application of ten arrays would be sufficient to reach this desired concentration.

#### **d. Conclusion**

This work had demonstrated the ability to load microneedles with an antibiotic, Ciprofloxacin, through the use of Ciprofloxacin crystals and through the loading of Ciprofloxacin in PLGA microparticles. Further investigation is needed to determine whether or not the loadings are sufficient as is, but regardless, there exists significant room for improvement in the loading. The biggest area is to capture the approximately 1 mg of loading capacity of the

microneedles. This will be best achieved through the use of microcrystals with increased concentration and increased uniformity in size.

## **IV. Conclusion**

### **a. Summary**

The results from this work are very promising to the eventual goal of using microneedles to deliver antiretrovirals and antibiotics. First, microparticles were synthesized and proved to be loading Saquinavir and Ciprofloxacin. Microcrystals were also synthesized for Ciprofloxacin. Microneedles were synthesized and showed loading of Saquinavir and Ciprofloxacin. It still remains unclear whether the loadings are sufficient for the intended applications, requiring further investigation.

### **b. Future work**

Although this work was a good step forward, there is still significant work in order to demonstrate the efficacy of using microneedles to deliver antiretrovirals and antibiotics. There exist two main areas to further this investigation. The first area is increasing the loading of the microneedles. Microcrystals show promise of achieving the entirety of the 1 mg loading limit of the microneedles. To further this limit, larger needles or potentially a reservoir driven device to deliver even more drug might be designed. The other main component left to be done is in vivo experiments to understand the concentrations of the plasma from the microneedle application. This can be done by applying microneedles loaded with drug and then measuring the concentration of the drug in the plasma at different time points.

If these measurements prove the presence of the drug in reasonable concentrations, the next step would be further investigation on the release characteristics of the drug. This would entail the use of different materials or suspension of the drug in various matrices of biodegradable materials. The ideal drug concentration in plasma over time would vary



depending on the drug and its intended use. The drug concentration profile over time would dictate the desired release of the drug. The third area of further research, after increasing the loading of the drug and measuring sufficient concentrations in vivo, would be not only to characterize the release characteristics of the drug, but to develop a system to allow tunable release. Since microcrystals demonstrate more promise due to higher loading capabilities, new mechanisms for controlled drug release need to be considered. One such idea would be to substitute the PAA matrix for various other biodegradable matrices in order to obtain the desired controlled release, while maintaining other characteristics, including mechanical stability. Another idea could complement the use of a reservoir to increase drug loading by developing the reservoir to allow for controlled release. This could include a specific release rate from the reservoir through the use of a selective membrane and osmotic pressure drive, thus allowing for tunable controlled release. There exist various methods of controlled release that could all be implemented in this system.

Achieving a high loading and controlled release microneedle system with demonstrated sufficient in vivo concentration measurements would be a huge advancement in the field of microneedle research. The work achieved thus far has laid the foundation for the future work to improve on the current system.

## **Acknowledgments**

This work could not have been possible without the dedicated efforts of a number of individuals. I would like to thank all of these individuals for their constant support throughout the entirety of this project. First, I would like to thank Peter DeMuth for his continued guidance and valued input during this project. Working with him on a regular basis was a pleasure and his mentorship helped guide me. I would also like to thank the rest of the Irvine lab for their help and expertise on various parts of this project. Next, I would like to thank Professor Irvine for his keen advice and generous support for this project as well as for his dedicated instruction in courses leading up to this project that helped prepare me to accomplish this project. Finally, I would like to thank all my family and friends for their unwavering support throughout the last four years.

## Works cited

- [1] Jain, Ashish. Microneedles: A revolution of Transdermal Drug Delivery. Pharmainfo.net. Posted Friday, May 2, 2008. Accessed April 27<sup>th</sup> 2012. <<http://www.pharmainfo.net/reviews/microneedles-revolution-transdermal-drug-delivery>>
- [2] Daugherty AL, Mrsny RJ. Emerging technologies that overcome biological barriers for therapeutic protein delivery. *Expert Opinion on Biological Therapy* 2003;3(7): 1071-81.
- [3] Nir Y, Paz A, Sabo E, Potasman I. Fear of injections in young adults: prevalence and associations. *American Journal of Tropical Medicine and Hygiene* 2003;68(3):341e4.
- [4] Ranjith Kumar et al., Review on Needle free drug delivery systems. *Int. J. Rev. Life. Sci.*, 1(2), 2011, 76-82
- [5] Gill H. S., Denson D. D., Burris B. A. & Prausnitz M. R. Effect of microneedle design on pain in human volunteers. *Clin J Pain* 24, 585–594 (2008).
- [6] Benjamin, David. Basic Pharmacology. Clinical Pharmacology. Accessed April 27<sup>th</sup>, 2012. <<http://www.doctorbenjamin.com/pharm/pharm.htm>>
- [7] Prausnitz MR, Langer R. Transdermal drug delivery. *Nat Biotechnol.* 2008;26:1261–1268.
- [8] Dezutter-Dambuyant C, Charbonnier AS, Schmitt D. [Epithelial dendritic cells and HIV-1 infection in vivo and in vitro]. *PatholBiol (Paris)*. 1995 Dec;43(10):882-8.
- [9] Piot P, Bartos M, Ghys PD, Walker N, Schwartlander B: The global impact of HIV/AIDS. *Nature* 2001, 410:968-973.
- [10] Panel of Clinical Practices for Treatment of HIV Infection, Guidelines for the use of antiretroviral agents to treat HIV infection in pediatric patients, *Pan. Am. J. PublicHealth* 10 (2001) 426–435.
- [11] C.A. Shah, Adherence to high activity antiretroviral therapy (HAART) in pediatric patients infected with HIV: issues and interventions, *Indian J. Pediatr.* 74 (2007)55–60.
- [12] LookChem. Saquinavir Basic Information. Accessed April 28<sup>th</sup> 2012. <<http://www.lookchem.com/Saquinavir/>>
- [13] Martin-Facklam M, Burhenne J, Ding R, et al. Dose-dependent increase of saquinavir bioavailability by the pharmaceutical aid cremophor EL. *Br J Clin Pharmacol.* 2002;53:576–81.
- [14] Gold Standard Inc. Saquinavir. Revised 12-9-2010. Accessed April 29<sup>th</sup> 2012. <[http://americareoncall.com/yahoo\\_site\\_admin/assets/docs/INVIRASE.53102229.pdf](http://americareoncall.com/yahoo_site_admin/assets/docs/INVIRASE.53102229.pdf)>
- [15] Vanhove GF, Kastrissios H, Gries JM, et al. Pharmacokinetics of saquinavir, zidovudine, and zalcitabine in combination therapy. *Antimicrob Agents Chemother.* 1997;41(11):2428–2432.
- [16] Boffito M., et al. 2005. Boosted saquinavir hard gel formulation exposure in HIV-infected subjects: ritonavir 100 mg once daily versus twice daily. *J. Antimicrob. Chemother.* 55:542–545.
- [17] AIDSinfo. Saquinavir mesylate. Last updated March 4, 2012. Accessed April 30<sup>th</sup> 2012. <<http://aidsinfo.nih.gov/drugs/164/saquinavir-mesylate/patient/>>

- [18] Back DJ, Khoo SH, Gibbons SE, et al. The role of therapeutic drug monitoring in treatment of HIV infection. *Br J Clin Pharmacol*. 2001;51:301–308.
- [19] Dickinson L, Boffito M, Khoo SH, et al. Pharmacokinetic analysis to assess forgiveness of boosted saquinavir regimens for missed or late dosing. *J Antimicrob Chemother* 2008;62:161-7.
- [20] RxList. Selzentry. The internet drug Index. Accessed May 1<sup>st</sup>, 2012. <<http://www.rxlist.com/selzentry-drug/indications-dosage.htm>>
- [21] Abel S, Russell D, Whitlock LA, Ridgway CE, Nedderman AN, Walker DK (April 2008). "Assessment of the absorption, metabolism and absolute bioavailability of maraviroc in healthy male subjects". *British Journal of Clinical Pharmacology* 65 (Suppl 1): 60–7. doi:10.1111/j.1365-2125.2008.03137.x
- [22] DrugBank. Maraviroc. Open Data Drug and Drug Target Database. Accessed May 1<sup>st</sup> 2012. <<http://www.drugbank.ca/drugs/DB04835>>
- [23] MacArthur RD, Novak RM. Reviews of anti-infective agents: maraviroc: the first of a new class of antiretroviral agents. *Clin Infect Dis*. 2008;47:236–241
- [24] ChinyereOkoli, Marco Siccardi, Sathish Thomas-William, NgoziDufty, Kirstin Khonyongwa, Jonathan Ainsworth, John Watson, Roseanne Cook, Kate Gandhi, Geraldine Hickinbottom, Andrew Owen, and Stephen Taylor. Once daily maraviroc 300 mg or 150 mg in combination with ritonavir-boosted darunavir 800/100 mg. *J. Antimicrob. Chemother.* 2011 : dkr493v1-dkr493
- [25] Ha H.R., Follath F., Bloemhard Y., Krahenbuhl S. Determination of saquinavir in human plasma by high-performance liquid chromatography . (1997) *Journal of Chromatography B: Biomedical Applications*, 694 (2) , pp. 427-433.
- [26] Van Heeswijk RP, Hoetelmans RM, Harms R, et al. Simultaneous quantitative determination of the HIV protease inhibitors amprenavir, indinavir, nelfinavir, ritonavir and saquinavir in human plasma by ion-pair high-performance liquid chromatography with ultraviolet detection. *J Chromatogr B Biomed Sci Appl*. 1998;719:159-168
- [27] RxList. Invirase. The Internet Drug Index. Accessed May 1<sup>st</sup>, 2012. <<http://www.rxlist.com/invirase-drug.htm>>
- [28] Sigma-Aldrich. Saquinavir-mesylate. Date accessed May 1<sup>st</sup>, 2012. <<http://www.sigmaaldrich.com/catalog/product/sigma/s8451?lang=en&region=US>>
- [29] Notari, S., Tommasi, C., Nicastri, E., Bellagamba, R., Tempestilli, M., et al. (2009) Simultaneous determination of maraviroc and raltegravir in human plasma by HPLC-UV. *IUBMB Life*, 61, 470–475.
- [30] Sigma-Aldrich. Maraviroc. Date accessed April 24<sup>th</sup>, 2012. <<http://www.sigmaaldrich.com/catalog/product/sigma/pz0002?lang=en&region=US>>
- [31] Gupta J, Felner EI, Prausnitz MR. Minimally invasive insulin delivery in subjects with type 1 diabetes using hollow microneedles. *Diabetes Technol Ther*. 2009;11:329–337
- [32] Borden Institute. Chapter 10: Infections. Accessed April 22<sup>nd</sup>, 2012. <[http://www.bordeninstitute.army.mil/other\\_pub/ews/Chp10Infections.pdf](http://www.bordeninstitute.army.mil/other_pub/ews/Chp10Infections.pdf)>

- [33] FDA. Cipro Tablets. 2004 Bayer Pharmaceuticals Corporation. Accessed April 24<sup>th</sup>, 2012. <<http://www.fda.gov/downloads/Drugs/EmergencyPreparedness/BioterrorismandDrugPreparedness/UCM130802.pdf>>
- [34] Kumar R, Aneja KR, Roy P, Sharma M, Gupta R, Ram S. Evaluation of minimum inhibitory concentration of quinolones and third generation cephalosporins to Salmonella typhi isolates. *Indian J Med Sci* 2002;56:1-8
- [35] Univgraph. Ciprofloxacine. Accessed May 1<sup>st</sup>, 2012. <<http://www.univgraph.com/bayer/inserts/ciprotab.pdf>>
- [36] Sigma-Aldrich. Ciprofloxacine. Accessed April 25<sup>th</sup>, 2012. <<http://www.sigmaaldrich.com/catalog/product/fluka/17850?lang=en&region=US>>
- [37] Arnold MM, Gorman EM, Schieber LJ, Munson EJ, Berkland C. NanoCipro encapsulation in monodisperse large porous PLGA microparticles. *J Control Release*. 2007;121:100–109.
- [38] Olivera ME, Manzo RH, Junginger HE, Midha KK, Shah VP, Stavchansky S, Dressman JB, Barends DM. 2010. Biowaiver monographs for immediate release solid oral dosage forms: Ciprofloxacine hydrochloride. *J Pharm Sci* 100(1):22–33
- [39] Patel SA, Patel NM, Patel MM. Simultaneous spectrophotometric estimation of Ciprofloxacine and Ornidazole in tablets. *Indian J Pharm Sci* 2006;68:665-7